ChemEngineering

Article

Solar Still Unit as a Component of Domestic Wastewater Treatment in Isolated Rural Communities: A Case Study in Colombia

Carlos Mauricio Meza [1], Franco Hernan Gomez [2,3,*], Kelly Cristina Torres [4], Oscar Orlando Porras [5], Alessandro Abbà [6], Marta Domini [6], Sabrina Sorlini [2,6] and Mentore Vaccari [2,6]

1 Research Group on Environmental Engineering (GIAS), Instituto Universitario de La Paz-UNIPAZ, Km 14, Vía B/Manga, Barrancabermeja 687031, Colombia; carlos.meza@unipaz.edu.co
2 Research Centre on Appropriate Technologies for Environmental Management in Resource Limited Countries (CeTAmb), University of Brescia, Via Branze 43, 25123 Brescia, Italy; sabrina.sorlini@unibs.it (S.S.); mentore.vaccari@unibs.it (M.V.)
3 Group on Governance of Climate Change (GGCC), Barcelona East School of Engineering, Universitat Politècnica de Catalunya—BarcelonaTech, Av. Maristany, 16, 08019 Barcelona, Spain
4 Research Group on Conservation and Use of Biodiversity—BioCon, Instituto Universitario de La Paz-UNIPAZ, Km 14, Vía B/Manga, Barrancabermeja 687031, Colombia; vicerectoria@unipaz.edu.co
5 Research Group on Innovation, Technological Development, and Competitiveness in Agribusiness Systems—GIADAI, Instituto Universitario de La Paz-UNIPAZ, Km 14, Vía B/Manga, Barrancabermeja 687031, Colombia; rectoria@unipaz.edu.co
6 Department of Civil, Environmental, Architectural Engineering and Mathematics, University of Brescia, Via Branze 43, 25123 Brescia, Italy; alessandro.abba@unibs.it (A.A.); marta.domini@unibs.it (M.D.)
* Correspondence: franco.gomez@unibs.it

Abstract

The use of non-conventional systems for domestic wastewater management has gained attention in rural areas of the Global South, where centralised infrastructure is often limited. This study presents the design, construction, and pilot-scale evaluation of a solar still unit operated under passive and photovoltaic-assisted active modes as a separation and polishing component for domestic wastewater from a rural site in Barrancabermeja, Colombia. Performance was assessed through physicochemical and microbiological characterisation of influent wastewater and treated condensate, together with hourly monitoring of distillate production, water temperature, glass-cover temperature, and ambient conditions. Under passive operation, a theoretical distillation model was applied, empirically adjusted, and evaluated using MAE, RMSE, MAPE, and R^2. Under the tested conditions, indicative within-mode reductions reached 80.9% and 89.3% for chemical oxygen demand (COD), 95.6% and 93.8% for biochemical oxygen demand (BOD_5), and 94.0% and 94.4% for total suspended solids (TSS) under passive and active modes, respectively. Microbial indicators showed minimum estimated reductions above 99.9%, with faecal coliforms reduced to very low levels in passive mode and not detected in the analysed active-mode condensate sample. Maximum daily condensate production reached 1.445 L m^{-2} day^{-1} in passive mode and 2.262 L m^{-2} day^{-1} in active mode, confirming the low-flow nature of the unit. Approximately 50% of daily production occurred between 12:00 and 15:00 h. The model reproduced the main diurnal production pattern, although empirical correction was required. Overall, the unit may improve condensate quality under pilot-scale conditions and shows potential as a polishing component within decentralised, low-flow treatment trains.

Keywords: wastewater; water quality; solar thermal; solar still; decentralised sanitation; rural; WASH technologies

Check for updates

Received: 26 April 2026
Revised: 12 June 2026
Accepted: 29 June 2026
Published: 7 July 2026

1. Introduction

In Latin America and the Caribbean, inadequate domestic wastewater treatment remains a leading cause of water pollution, particularly in rural areas where infrastructure is often limited or nonexistent. A significant number of communities still rely on septic tanks or informal solutions, with only a small proportion connected to formal wastewater collection systems [1–4]. In Colombia, this challenge is reflected in national statistics: in 2024, only 36.71% of the total wastewater discharged through sewage systems was treated before reaching natural water bodies, corresponding to 30.8 $m^3 s^{-1}$ [5]. According to the 2024 sectoral report, Colombia recorded 729 wastewater treatment systems (WWTS/STAR) linked to sewerage systems. Among the 415 wastewater treatment plants (WWTPs/PTAR), 114 had installed capacities above 50 L s^{-1}, while the remainder were below that threshold. Treatment was dominated by secondary systems (72.6%; 529 systems), followed by systems with no available technology information (16.9%; 123), primary treatment (6.3%; 46), tertiary treatment (2.6%; 19), and preliminary treatment (1.7%; 12) [6]. In this context, achieving the 2030 Sustainable Development Goal 6 target of 68.6% urban wastewater treatment will require the implementation of alternative and decentralised treatment technologies, particularly in areas where conventional infrastructure remains limited [6,7]. Recent policy initiatives and planning instruments have increasingly encouraged resource efficiency, reuse, and sustainability in water and sanitation services, creating a favourable context for exploring decentralised treatment alternatives [8–10].

Solar still units offer a promising alternative for decentralised wastewater treatment in regions without access to conventional treatment systems. These systems harness solar energy to evaporate and condense water, thereby replicating the natural hydrological cycle. As a result, they can remove a wide range of contaminants, including dissolved salts, organic matter, and pathogenic microorganisms [11–13]. However, solar still technologies have been primarily developed and optimised for desalination and potable water production from saline or brackish sources. Most investigations have focused on improving thermal performance, increasing freshwater productivity, and enhancing condensation efficiency through structural modifications or advanced materials [14,15]. Design improvements such as external condensers, thermoelectric modules, nanofluids, and modified absorber geometries have been widely explored to increase yield and overall efficiency [16,17]. Recent studies have explored thin-film photothermal materials and porous bilayer structures to localise heat at the evaporation interface, thereby reducing thermal losses to the bulk water and enhancing solar-to-steam conversion performance [18,19]. These developments have enhanced evaporation rates; however, their primary application remains desalination rather than domestic wastewater treatment.

Solar still unit can be classified as passive or active. Passive systems rely on direct solar radiation, whereas active systems incorporate external heat sources or thermal storage materials to enhance performance [20]. Technological advancements have introduced design variations such as single-effect and multi-effect solar stills. In multi-effect systems, the latent heat of condensation is reused to drive subsequent evaporation stages, thereby improving energy efficiency [21,22]. Furthermore, the integration of phase change materials (PCMs), nano-enhanced PCMs, and structural elements such as thermal grids has demonstrated the potential to increase water production by 25% to over 300%, depending on the system configuration [23,24]. Solar distillation has also been evaluated for certain wastewater streams, including sewage water and reverse osmosis reject [25], while hybrid household-scale systems have been proposed for small-scale wastewater reuse [26]. Therefore, the research gap does not lie in the complete absence of studies on solar stills for wastewater treatment [27,28], but rather in the limited evidence regarding their use as polishing units within decentralised domestic wastewater treatment trains under rural tropical conditions.

https://doi.org/10.3390/chemengineering10070086

In this context, the selected configuration was designed as a low-cost pilot-scale system combining pre-filtration, passive solar distillation, and photovoltaic-assisted operation to assess its potential role as a polishing component under rural tropical conditions [24–26].

The objective of this study was to evaluate the pilot-scale design, construction, and performance of a solar still unit for domestic wastewater treatment under local rural conditions. The unit operates in both passive and active modes, depending on solar availability and external energy inputs. Rather than establishing full implementation feasibility, the study provides an initial assessment of treatment efficiency and operational performance in a rural setting. By focusing on low-cost, sustainable solutions adapted to local conditions, this study contributes to the broader goals of environmental protection, water resource conservation, and the advancement of appropriate technologies within a circular economy framework. This study contributes to this gap by evaluating the pilot-scale use of a solar still unit as a polishing component within a decentralised domestic wastewater treatment train under rural tropical conditions, combining water-quality assessment, passive–active operation, and thermal-performance analysis.

2. Materials and Methods

2.1. Location of the Study

The research was conducted in the rural area of the Barrancabermeja district, Santander, Colombia, at the Santa Lucia Research Center of the Universidad de la Paz (UNIPAZ), located at kilometre 14 on the left margin of the Barrancabermeja–Bucaramanga Road, in the village of El Zarzal (Figure 1, Table 1).

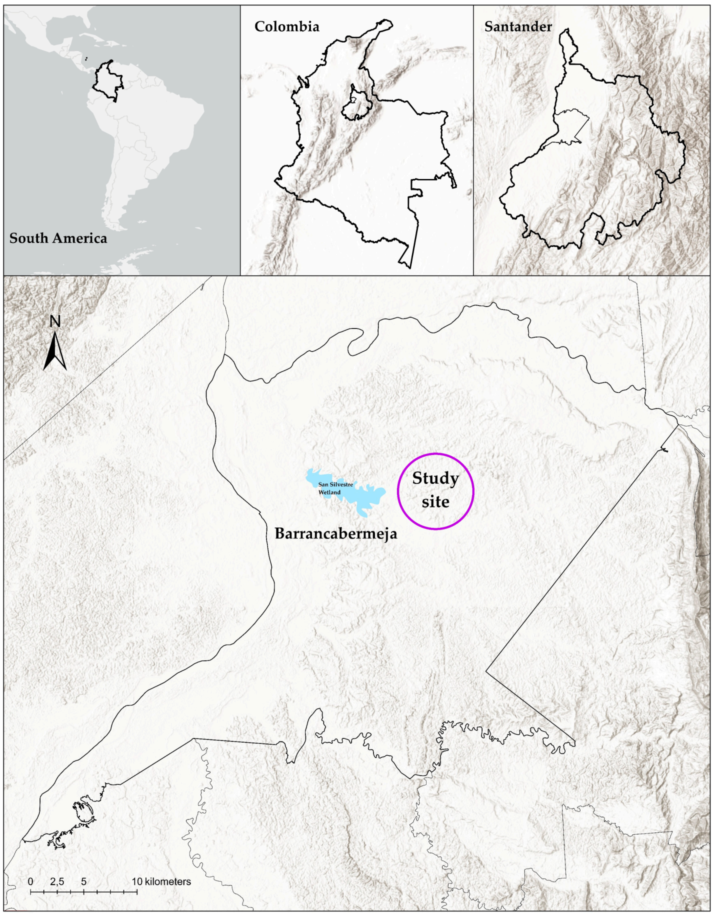

Figure 1. Location of the study area in rural Barrancabermeja, Santander, Colombia.

Table 1. Location and local environmental conditions [29,30].

Latitude	7.0689°
Longitude	−73.7451°
Meteorological Conditions	
Mean temperature	26–28 °C
Relative humidity	79%
Annual precipitation	3000 mm $year^{-1}$
Mean daily solar radiation	4.0–4.5 kWh m^{-2}
Sunshine duration	6 h day^{-1}

The study area is located in the rural zone of Barrancabermeja, Santander, within the biogeographical context of the Colombian Middle Magdalena Valley. This territory is characterised by lowland landscapes, aquatic systems associated with marshes, streams and wetlands, fragmented forest cover, agricultural areas and remnants of natural vegetation. From an environmental perspective, it shares ecological conditions with the San Silvestre Wetland Regional Integrated Management District—DRMI—a protected area declared by the Regional Autonomous Corporation of Santander through Agreement No. 00058 of 2006. According to Holdridge's life zone classification, the predominant formation is Tropical Humid Forest—bh-T—with elevations ranging from 70 to 255 m a.s.l., annual precipitation between 2500 and 3000 mm, and mean temperatures of 26–28 °C. These conditions support strategic ecosystems for hydrological regulation, ecological connectivity and biodiversity conservation [31].

2.2. Assessment Methodology Framework

The process for the design, implementation, and performance evaluation of a solar still unit for the treatment of domestic wastewater was carried out in three phases:

Phase A: Development of the pilot unit: This phase involves selecting the design parameters and components best suited to the Solar Still Unit (SSU) for domestic wastewater treatment.

Phase B: System construction: This phase includes the construction and monitoring of the SSU.

Phase C: Treatment-performance assessment and monitoring: This phase includes the characterisation of the wastewater to be treated and the evaluation of pollutant removal efficiency.

2.3. Phase A: Pilot-Scale SSU Design

The design parameters were based on those proposed by Patel et al. [32], including the system configuration, water depth, and construction materials. In addition, a pretreatment module was implemented using a filtration system, which helped reduce the presence of suspended solids within the solar collector.

2.4. Phase B: Construction of the Solar Still

The pilot solar still unit was constructed using the following components: (1) a steel support frame for the filtration unit, including a 20 L tank positioned approximately 1.2 m above the ground and connected to the solar collector by a pipe; (2) a galvanised zinc still chamber sealed with silicone; (3) a drainage system with 0.5 inch polyvinyl chloride (PVC) pipes designed to maintain a constant water depth (~2 cm); (4) an interior-mounted glass cover with rubber insulation to ensure thermal efficiency and airtightness; (5) a photovoltaic-powered electric resistor for active-mode operation; and (6) a bottom channel to collect the distilled water in a container. The unit operates in two configurations: passive mode, which uses solar radiation as the sole energy source, and active mode, enhanced by photovoltaic power to energise a heating resistor. Both modes include a filtration unit composed of coarse gravel, fine gravel, and sand; a galvanised still chamber; a transparent glass cover for solar capture; and a water collector. The active mode integrates a photovoltaic panel and electrical system to increase thermal efficiency and distillate yield.

During operation, the pre-filtration unit helped reduce suspended solids entering the still chamber, thereby limiting short-term fouling of the evaporation surface. After each operational run, the still chamber and glass cover were visually inspected and manually cleaned to remove residual solids, deposits, or biofilm accumulation. The use of galvanised zinc, PVC piping, glass, and silicone sealing was selected to support low-cost construction and basic material durability under pilot-scale conditions. However, long-term material degradation, scaling, fouling progression, and cleaning frequency were not systematically evaluated and should be addressed in future extended operation studies.

2.5. Phase C: Solar Still Unit Efficiency and Monitoring

The solar still unit was evaluated through four operational runs under passive mode and four operational runs under active mode. Each run corresponded to one full monitoring day, with hourly measurements recorded from 08:00 to 17:00 h. These runs were used to describe operational trends in thermal behaviour and distillate production. Domestic wastewater (DWW) samples were collected weekly at the inlet pipe of the septic tank located within the UNIPAZ facilities, prior to the wastewater entering the tank. The collected influent corresponded to mixed domestic wastewater generated from sanitary services and general facility activities within the campus. A single grab sample was obtained during each sampling event to characterise the raw influent conditions. Samples were transported to the Environmental Engineering Laboratory at UNIPAZ for analysis. Meteorological variables such as ambient temperature and relative humidity were obtained from the on-campus meteorological station, while cloud cover conditions were assessed through direct visual observation and field records during the experimental period.

Unit-related variables were monitored hourly, including water temperature and inner glass surface temperature, both measured using a calibrated digital thermometer. In addition, the hourly distillate volume was recorded during each experimental run.

Physicochemical and microbiological parameters were evaluated in raw domestic wastewater collected at the inlet of the septic tank and in the treated effluent obtained from the solar still unit. For each operating mode, an independent homogenised grab sample was used, reflecting the temporal variability of domestic wastewater generated under real conditions and limiting direct comparison of removal efficiencies between passive and active modes. No analytical replicates were available for the water-quality parameters evaluated in this study. The analysed parameters included total suspended solids (TSS), biochemical oxygen demand (BOD_5), and chemical oxygen demand (COD), determined according to Standard Methods 2540 D, 5210 B, and 5220 C of the Standard Methods for the Examination of Water and Wastewater [33], pH (HANNA HI 98127 pH meter, HANNA Instruments, Bogota, Colombia),, dissolved oxygen (DO) measured with a HANNA HI 9146 DO probe (HANNA Instruments, Bogotá, Colombia), electrical conductivity using a HANNA HI 9829 multiparameter probe (HANNA Instruments, Bogotá, Colombia), apparent colour (HANNA HI 727 colourimeter, HANNA Instruments, Bogotá, Colombia), and faecal and total coliforms determined by the membrane filtration technique.

The physicochemical values obtained for both the influent and the treated effluent were compared with the reference limits established in Colombian environmental regulations to assess treatment performance and compliance with discharge standards [34].

The efficiency of the solar still unit was evaluated in three ways:

2.5.1. Passive and Active Mode Performance

Solar still unit efficiency under passive and active modes, which included the analysis of temperature behaviour within the solar still in both configurations, as well as the productivity based on the volume of distilled water obtained.

2.5.2. Contaminant Removal Assessment

Contaminant removal efficiency of the solar still unit, determined by evaluating the changes in the concentration of the physicochemical and microbiological variables described in the previous section (Equation (1)).

$$\text{Removal Efficiency (\%)} = ((Cc_{in} - Cc_{out})/Cc_{in}) \times 100 \quad (1)$$

where

Cc_{in}: concentration of the parameter in the influent stream of the treatment unit (mg L^{-1});
Cc_{out}: concentration of the parameter in the effluent stream of the treatment unit (mg L^{-1}).

2.5.3. Thermal Analysis of Distillate Production

In addition to the experimental evaluation, the performance of the solar still was analysed using a theoretical model of water distillation proposed by Medugu, D. W., and Ndatuwong, and Gupta et al. [35,36]. The analysis was restricted to the passive mode of operation, as this configuration represents the intrinsic thermal response of the system without external energy inputs. This allows the isolation of the fundamental heat and mass transfer processes governing evaporation and condensation, which form the basis for both passive and assisted (active) configurations.

The theoretical distillate production was calculated through a sequential process that links thermal conditions with mass transfer mechanisms within the solar still according to the following logic:

$$\text{Tw, Tg} \rightarrow \text{Pw, Pg} \rightarrow \text{hcw} \rightarrow \text{hew} \rightarrow \text{Wsim}$$

where

Tw: temperature of the basin water (°C);
Tg: temperature of the inner glass cover (°C);
Pw: saturation vapour pressure at water temperature (Pa);
Pg: saturation vapour pressure at glass temperature (Pa);
hcw: convective heat transfer coefficient between water and glass (W m^{-2} $°C^{-1}$);
hew: evaporative heat transfer coefficient (W m^{-2} $°C^{-1}$);
Wsim: theoretical distillate production (mL m^{-2} h^{-1} or mL m^{-2} day^{-1}).

Distillate productivity was normalised to the effective evaporation area of the solar still unit. In this pilot unit, the effective evaporation area corresponded to the exposed basin area used for evaporation, which was approximately 1 m^2.

Model calibration: To account for real system inefficiencies, a correction factor k was introduced (Equation (2)):

$$\text{Wsim\_k} = \text{k} \cdot \text{Wsim} \quad (2)$$

where Wsim_k is the adjusted model output, and k represents the effective operational efficiency of the system, integrating unmodelled processes such as heat losses, incomplete condensation, and internal thermal storage.

Preliminary model performance was assessed using MAE, RMSE, MAPE, and R^2. These indicators allow the assessment of both accuracy and bias of the model predictions [37].

3. Results

3.1. Phase A and B: Development and Construction SSU

The proposed configuration and main design features of the solar still unit (SSU) are presented in Figure 2. In addition, key factors such as meteorological conditions, ease of operation and maintenance, availability of materials, and construction costs were taken into account to ensure the continuous and reliable operation of the unit. A brief description of the components and dimensions of the solar still unit is provided in Table 2.

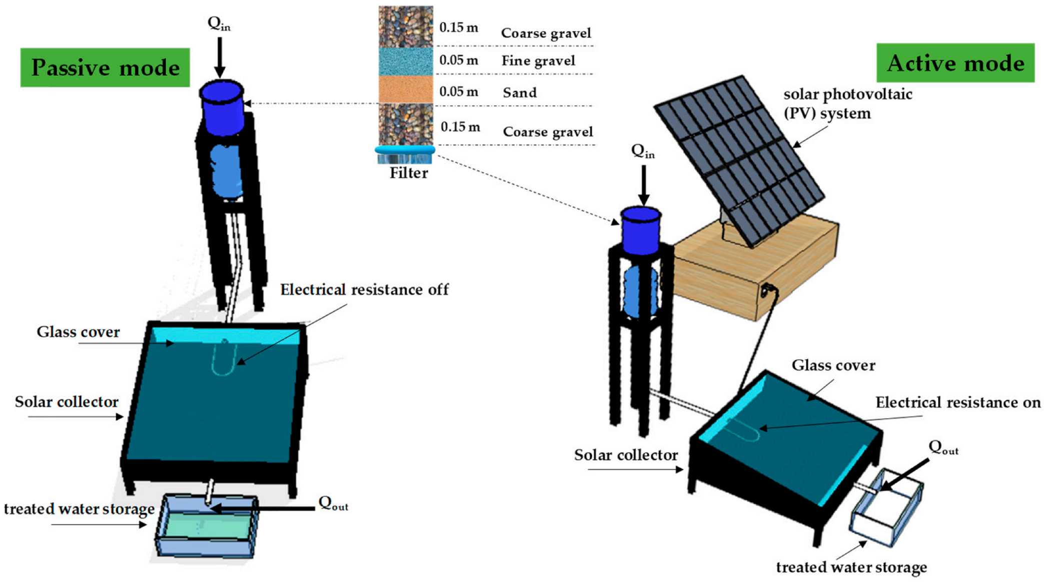

Figure 2. Schematic representation of the solar still unit in passive and active modes. The unit combines pre-filtration, solar-driven evaporation, condensation on the inclined glass cover, and distillate collection; in active mode, a photovoltaic-powered heater provides auxiliary heat input.

Table 2. Technical specifications of the solar still unit.

Component	Image	Description
Filter	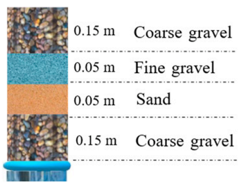	The system is composed of three granular layers: 0.15 m of coarse gravel (DN: 4.75 mm), 0.05 m of fine gravel (DN: 2.36 mm), and 0.05 m of sand (DN: 0.075 mm); nominal diameter (DN).
Glass cover	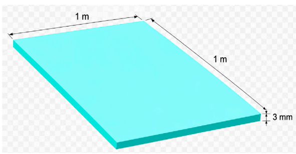	The unit incorporates a hermetically sealed 3 mm thick transparent glass cover that creates a greenhouse effect inside the solar collector, promotes condensation, and, owing to its inclined arrangement, enables the collection of distilled water into the treated-water storage container.
Solar collector	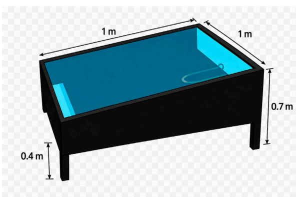	The solar collector was constructed using 1 m × 1 m (length × width) galvanised zinc sheets. The lower support structure has a height of 0.4 m, while the upper support structure has a height of 0.7 m, providing a 15° inclination to the cover.

https://doi.org/10.3390/chemengineering10070086

Table 2. *Cont.*

Component	Image	Description
Treated water storage	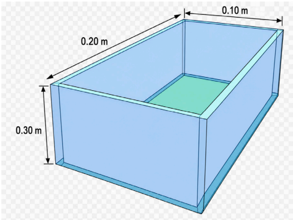	A transparent plastic container with a capacity of 6 L was used for the storage of treated wastewater. The container had dimensions of 0.30 m in height, 0.10 m in width, and 0.20 m in length.
Electrical resistance		A 75 W 220 V^{-1} electric immersion resistance was used, capable of converting electrical energy into thermal energy and reaching temperatures of up to 100 °C, considering the capacity of the existing photovoltaic panels.
Solar photovoltaic (PV) system	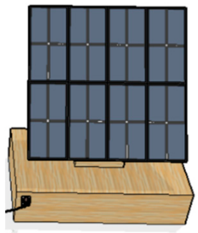	The system comprises six 270 W photovoltaic panels, a 24 V DC distribution panel, and a 1 kWh battery, which provide the electrical energy required to operate the heating element and ensure continuous operation of the solar still unit.

The domestic wastewater treatment unit operated as designed, allowing the controlled transfer of wastewater through the filtration and solar still units. The influent domestic wastewater entered the filter unit, where suspended solids were reduced, contributing to a decrease in fouling and maintenance requirements of the solar collector.

After filtration, the wastewater was conveyed to the solar still unit via PVC piping. Within the solar collector, the combined effect of solar radiation (passive mode) and the electric heating element powered by the photovoltaic system (active mode) resulted in a progressive increase in water temperature, leading to the generation of water vapour. Condensation occurred on the inclined glass cover, where droplets flowed by gravity and were collected in the distilled water container.

The treated effluent obtained from the distillation process was analysed in the laboratory. The results were assessed in accordance with the applicable legal standards, allowing the evaluation of the unit's performance in terms of wastewater treatment efficiency.

3.2. Phase B and C: Solar Still Unit Efficiency Under Passive and Active Modes

The monitored variables, glass temperature (Tg), water temperature (Tw), ambient temperature (Ta), and distillate volume (W), exhibited distinct temporal patterns under passive and active operating modes throughout the evaluation period. The temperature profiles exhibited consistent diurnal behaviour under both operational modes. Ambient temperature (Ta) increased from morning hours, reaching maximum values between 13:00 and 14:00 h, and declining thereafter. Water temperature (Tw) followed a similar but amplified pattern, exceeding ambient conditions due to solar heat absorption and internal thermal accumulation. Glass surface temperature (Tg) remained lower than Tw throughout the operational period, maintaining the temperature gradient required for condensation (Figure 3).

(**a**)

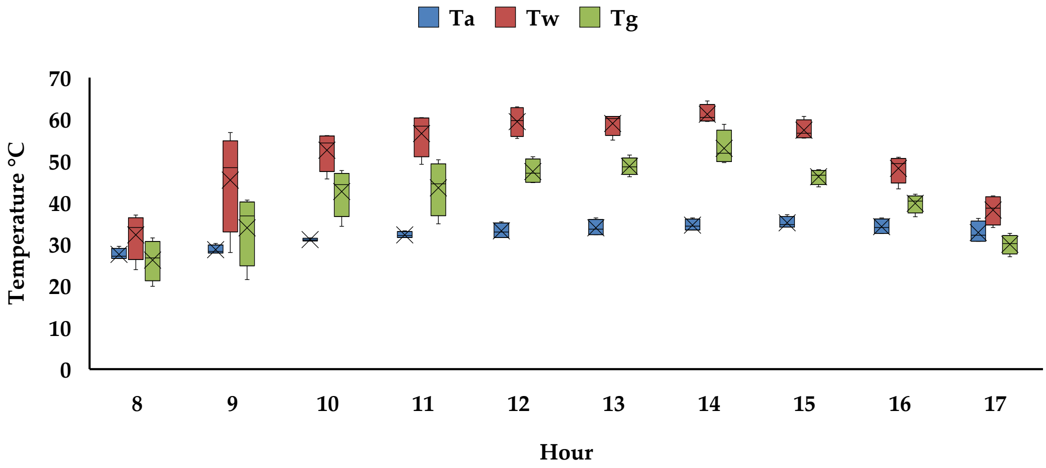

(**b**)

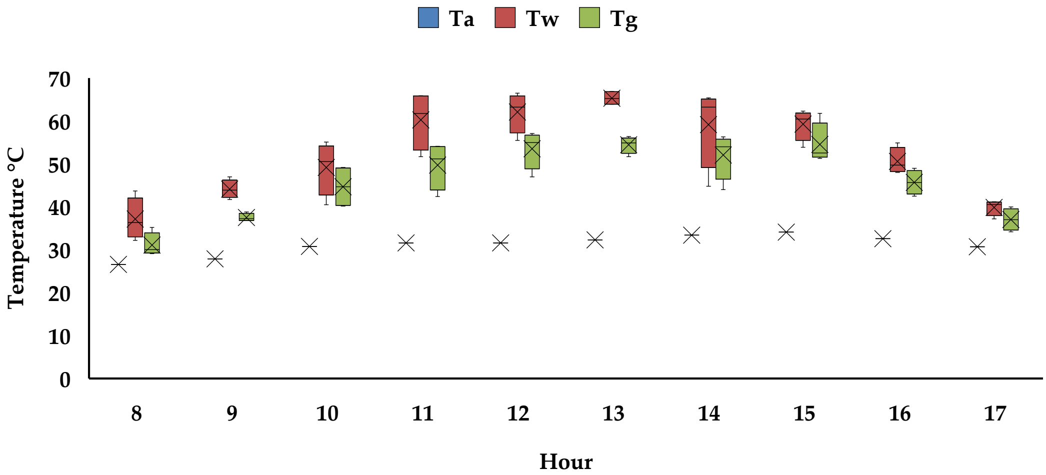

Figure 3. Hourly variation in ambient, water, and glass-cover temperatures under passive and active operating modes. (**a**) Passive mode and (**b**) active mode, monitored from 08:00 to 17:00 h.

Under passive operation, the difference between Tw and Tg peaked around midday, coinciding with maximum distillate production. However, temperature fluctuations were more pronounced during late afternoon hours. In contrast, the active mode exhibited higher Tw values and a more stable thermal gradient between Tw and Tg during peak solar hours. This enhanced thermal stability may have contributed to sustained evaporation rates and higher observed distillate production. Overall, the thermal behaviour confirms the direct relationship between water temperature elevation, vapour pressure increase, and hourly distillate yield.

The graphical analysis of the four experimental days shows that distillate production in both operational modes followed a consistent diurnal pattern, increasing from 08:00 h, reaching maximum values between 12:00 and 14:00 h, and declining thereafter. This trend reflects the direct influence of solar radiation intensity and internal thermal accumulation within the unit (Figures 4 and 5).

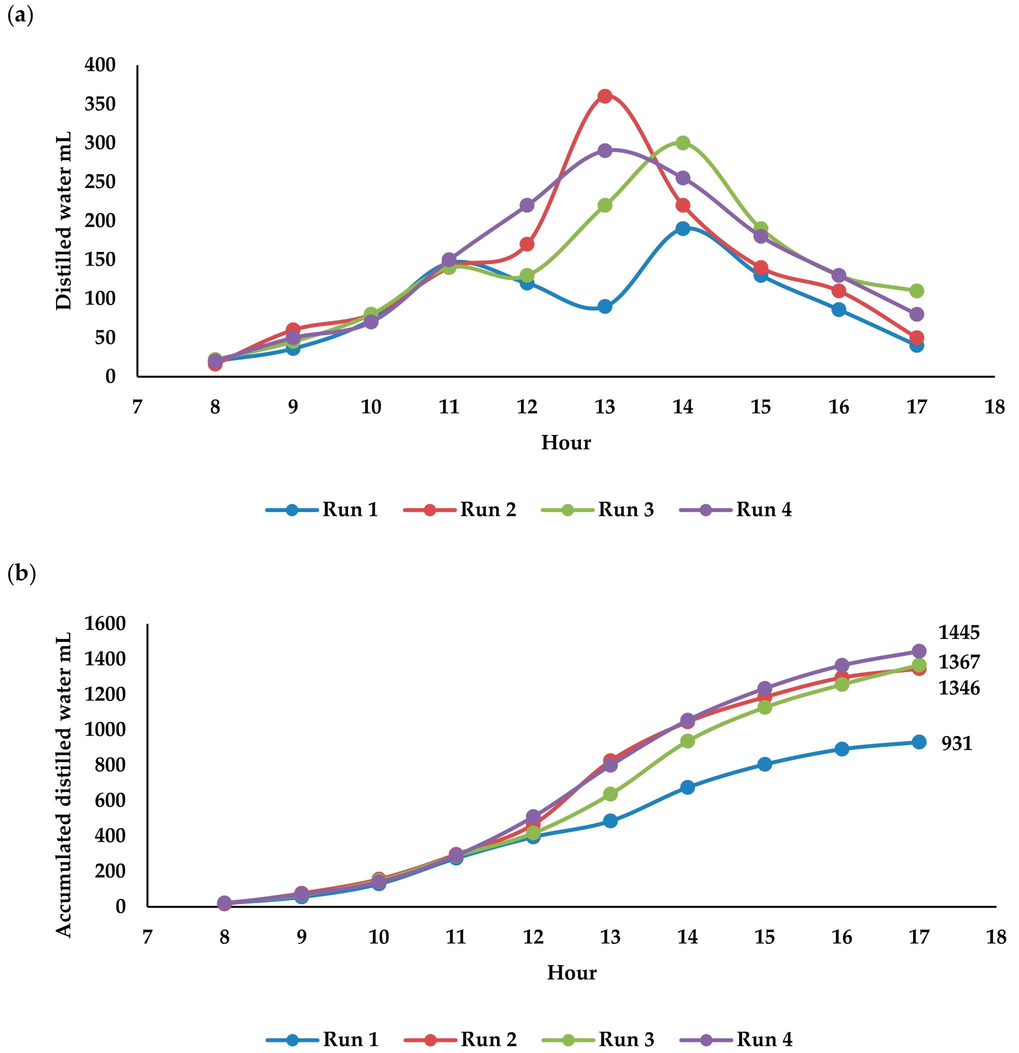

Figure 4. Distillate production under passive operating mode: (**a**) hourly production and (**b**) cumulative production from 08:00 to 17:00 h.

Under passive operation, production peaks were sharp and concentrated within a narrower time window, with noticeable variability between days, indicating strong dependence on instantaneous meteorological conditions. Maximum hourly outputs ranged between 280 and 360 mL during peak radiation hours, followed by a rapid decline after 15:00 h. In contrast, the active-mode unit exhibited higher and more sustained production levels, with peak hourly values of approximately 330–350 mL and a smoother late-afternoon decline. Under the tested conditions, the active configuration showed higher and more stable distillate production than the passive mode, suggesting that auxiliary photovoltaic-powered heating may improve short-term thermal stability and water yield.

The maximum daily treated water production reached 1445 mL m^{-2} day^{-1} in passive mode and 2262 mL m^{-2} day^{-1} in active mode. The higher productivity observed in active mode reflects the contribution of additional energy input, which enhances evaporation rates beyond conventional passive configurations.

Meteorological variability further illustrates this contrast. Under increased cloud cover, passive-mode production decreased to 931 mL m^{-2} day^{-1}. In contrast, during run 1, despite light rainfall throughout the day, the active mode maintained a production of 1380 mL m^{-2} day^{-1} (Figure 6). The observed distillate production confirms the low-flow nature of the solar still unit. Therefore, the unit should not be interpreted as a stand-alone option for treating the full domestic wastewater volume generated by a household. Its practical application would be more realistic as a polishing component for selected low-flow streams or as part of a modular decentralised treatment train.

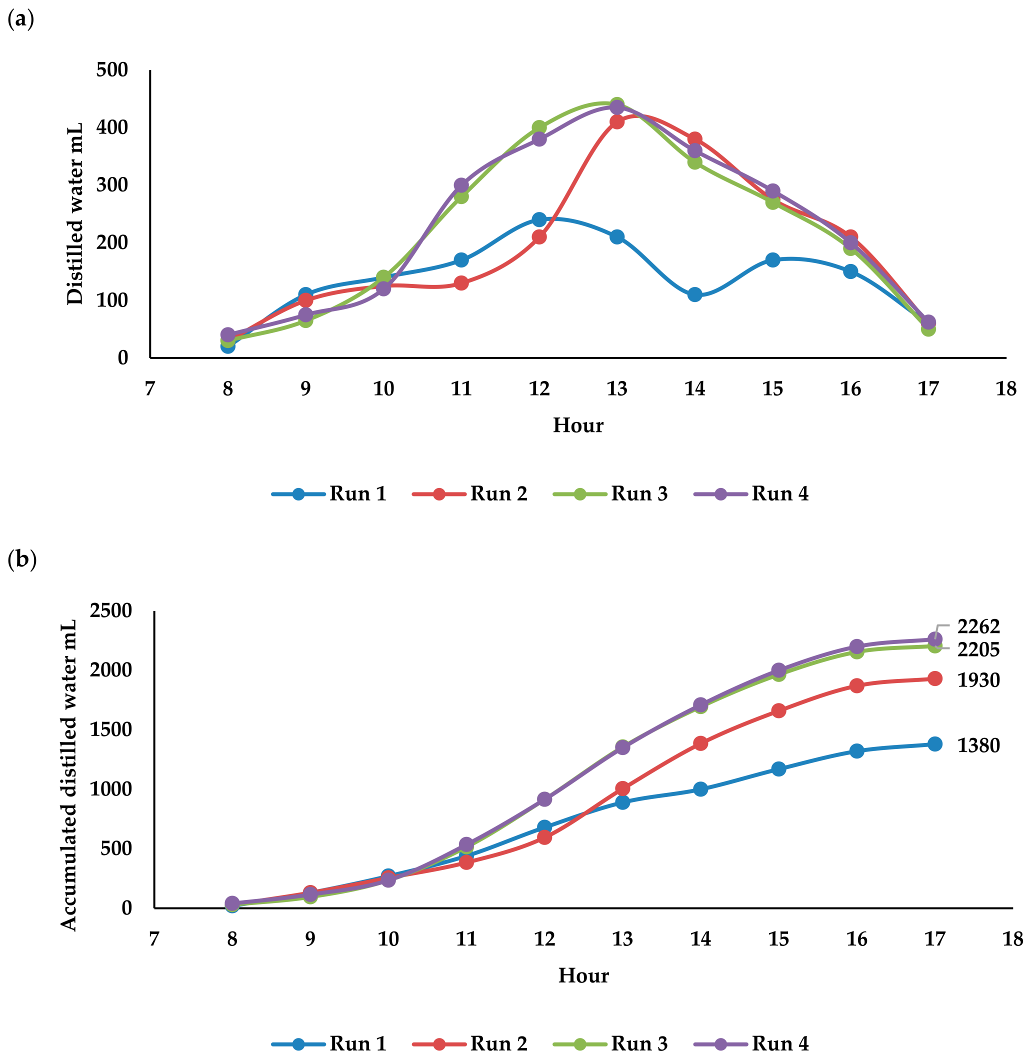

Figure 5. Distillate production under active operating mode: (**a**) hourly production and (**b**) cumulative production from 08:00 to 17:00 h.

Furthermore, the active mode enhanced distillate production compared to the passive configuration throughout most of the operational period. Hourly production increased from 08:00 h onward in both modes, reaching maximum values between 13:00 and 14:00 h, which coincides with peak solar radiation and maximum thermal accumulation within the system.

The highest relative improvement was observed at 12:00 h, where active operation produced approximately 92% more distillate than the passive mode. In passive operation, production exhibited a pronounced peak concentrated around 13:00–14:00 h, with nearly 38% of the total daily yield occurring within this two-hour interval. This indicates strong dependence on instantaneous solar intensity.

In contrast, the active configuration not only increased total production but also broadened the high-efficiency window. Nearly 50% of the total daily distillate under active operation was generated between 12:00 and 14:00 h, and elevated production levels were sustained from 12:00 to 15:00 h. This more uniform distribution suggests that auxiliary energy input may have supported greater thermal stability, reduced short-term sensitivity to solar-radiation fluctuations, and contributed to a longer effective production period and higher observed cumulative yield.

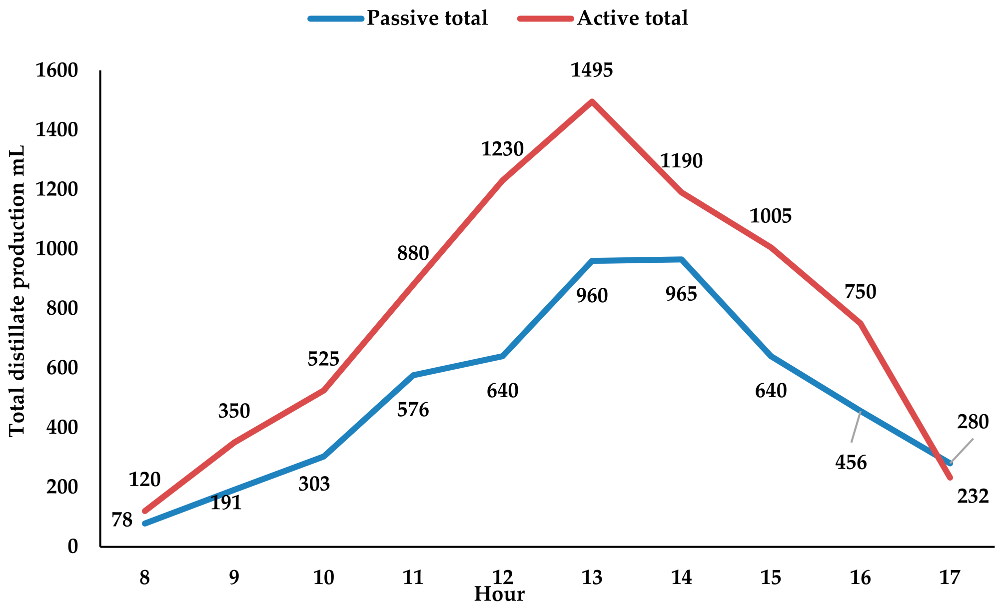

Figure 6. Hourly distillate production under passive and active operating modes.

A comparison of the data collected during the SSU runs under passive and active operating modes revealed a clear relationship between the recorded water temperature (Tw) and the glass cover temperature (Tg) in both modes of operation, which influenced the total volume of treated water produced (Figure 7). When the water reached the temperature required for phase change but the condensation surface (Tg) exhibited an equal or higher temperature, the pilot system efficiency decreased due to reduced condensation rates, resulting in a lower volume of treated water.

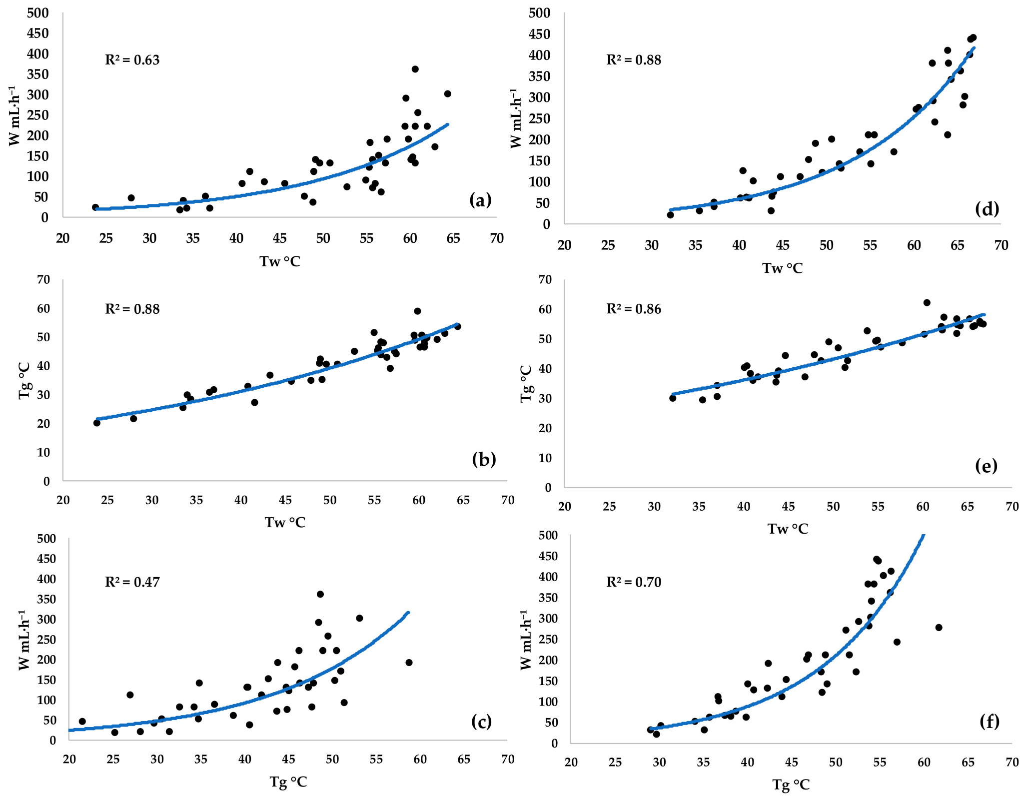

Figure 7. Relationships between hourly distillate production and thermal variables under passive (**a**–**c**) and active (**d**–**f**) operating modes.

Distillate production (W) exhibited a strong positive correlation with water temperature (Tw) and with the thermal gradient between water and glass (Tw–Tg), as supported by the linear trendlines and corresponding coefficients of determination (R^2) presented in the graphical analysis. Under active operation, an average Tw of 53 °C ± 10.5 was recorded, compared to 51 °C ± 10.5 in passive mode. Although the difference in mean temperature between modes was small and not statistically pronounced across individual runs, the active configuration maintained a more stable thermal regime throughout each operational cycle.

In this pilot study, this enhanced thermal consistency appears to have supported sustained Tw–Tg differentials during peak hours, contributing to higher observed cumulative distillate yield. The findings suggest that evaporation–condensation performance was influenced not only by absolute Tw values, but also by the persistence and stability of the Tw–Tg thermal gradient.

Finally, the active mode used a 75 W immersion heater supplied by the photovoltaic system. Assuming continuous operation during the 10 h monitoring period, the theoretical electrical demand of the heater would be approximately 0.75 kWh day^{-1}. Based on the maximum observed active-mode production of 2.262 L m^{-2} day^{-1} and an effective evaporation area of approximately 1 m^2, this corresponds to an indicative productivity of approximately 3.0 L kWh^{-1} and a specific energy demand of approximately 0.33 kWh L^{-1}. However, actual electrical consumption, photovoltaic conversion efficiency, battery losses, and cost-performance indicators were not directly measured. These values are theoretical estimates based on nominal heater power and observed condensate production, not experimentally validated energy-efficiency measurements.

3.3. Phase B and C: Pollutant Removal Efficiency

The physicochemical and microbiological results indicated substantial reductions in several measured parameters under both passive and active operating modes (Table 3). However, because passive and active modes were evaluated using different influent wastewater samples and water-quality characterisation was based on single-point samples for each mode, and influent COD, BOD_5, TSS, and microbial concentrations differed between modes due to the temporal variability of domestic wastewater generated under real conditions, the reported removal efficiencies should be interpreted as indicative within-mode reductions, rather than as direct comparisons of treatment performance between passive and active operation. COD reductions of 81.0% and 89.2% were observed under passive and active configurations, respectively, while BOD reductions reached 95.6% and 93.8%.

These results indicate a substantial decrease in oxygen-demanding substances in the condensate after the evaporation–condensation process. However, these reductions should be interpreted as improvements in condensate quality associated with phase-change separation, rather than as evidence of organic matter mineralisation, since TOC was not measured. Dissolved oxygen (DO) increased to 2.05 mg L^{-1} and 2.09 mg L^{-1} in the treated samples, supporting the observed improvement in measured water-quality conditions. Total suspended solids (TSS) removal exceeded 94% in both modes (94.0% passive; 94.4% active). The evaporation–condensation mechanism prevents the transfer of non-volatile solids to the distillate phase, explaining the high separation efficiency observed. Electrical conductivity reductions of 91–92% further indicate substantial removal of dissolved constituents, while the marked decrease in apparent colour confirms the elimination of dissolved and colloidal substances. The treated effluent maintained pH values within the regulatory range (6.0–9.0), ensuring compliance with environmental discharge standards.

Table 3. Physicochemical and microbiological characteristics of influent and effluent domestic wastewater DWW.

			Passive Mode			Active Mode			Asadi et al., 2013 [38]			Igoud et al., 2020 [39]			Yusof et al., 2022 [40]			Kumar et al., 2025 [41]			Kumar et al., 2025 [42]		
Parameters	**Units**	**Ref.**	**U**	**T**	**Re%**	**U**	**T**	**Re%**	**U**	**T**	**Re%**	**U**	**T**	**Re%**	**U**	**T**	**Re%**	**U**	**T**	**Re%**	**U**	**T**	**Re%**
COD	mg O_2 L^{-1}	200	121	23	80.99	862	92	89.33	342.9 ± 44.32	44.6 ± 10.67	86.99	2580 ± 11	586 ± 7	77.3	84	8.6	89.76	50.3	29.4	41.55	923.40 ± 31.6	36.70 ± 0.92	96.02
BOD_5	mgO_2 L^{-1}	90	69.8	3.1	95.56	480	30	93.75	-	-	-	2150 ± 10	352 ± 8	83.6	18.06	0.3	98.34	2.9	1.6	44.82	512.70 ± 22.1	13.80 ± 0.32	97.3
DO	mg O_2 L^{-1}	N/A	0	2.05	-	0	2.09	-	-	-	-	-	-	-	-	-	-	2.3	2.4	-	-	-	-
TSS	Mg L^{-1}	100	167	10	94.01	354	20	94.35	120.6 ± 68.21	2.2 ± 1.31	98.17	2850 ± 11	0 ± 0	100	176	2.6	98.52	827	382	53.80	425.40 ± 21.9	28.80 ± 4.48	95.1
Conductivity	μs cm^{-1}	N/A	1452	126.9	91.26	1636	129	92.12	-	-	-	2830 ± 12	15.8 ± 0.5	99.44	160.2	44.4	72.28	-	-	-	1212.32 ± 2.1	156.50 ± 0.18	88.5
Apparent colour	Colour units	N/A	410	20	95.12	315	25	92.06	-	-	-				-	-	-	4.9	1.2	75.51	-	-	-
pH	pH	6.00–9.00	6.48	7.59	-	7.20	8.16	-	7.2 ± 0.29	7.8 ±0.24	-	7.3 ± 0.3	8.9 ± 0.3	-	7.42	6.9	-	8.3	7.0	-	7.04 ± 0.02	7.28 ± 0.04	-
Total coliforms	CFU 100 mL^{-1}	N/A	>24 × 10^4	220	99.90	360 × 10^5	20 × 10^2	99.99	-	-	-	>310^4	0	100	1020	8.3	99.18	-	-	-	10^7–10^9	≤100	100 *
Faecal coliforms	CFU 100 mL^{-1}	N/A	>24 × 10^4	2	99.99	40 × 10^5	0	100	-	-	-	>310^4	0	100	110	2.6	97.64	-	-	-	-	-	-

Note: Ref.: Reference values according to Colombian Resolution 631 of 2015. U: Wastewater Untreated; T: Wastewater Treated; Re%: Removal Efficiency (%); N/A: Not applicable; Microbial Re% values based on influent concentrations reported as (>) represent minimum estimated removals; 0 indicates non-detection in the analysed sample. * Total coliform (MPN·100 mL^{-1}).

The results indicated substantial microbial reduction under both operating modes. Total coliform removal was above 99.90%, while faecal coliforms were reduced to very low or non-detectable levels in the samples of treated water (100% removal).

3.4. Estimation of Distillate Production

The hourly distillate production was compared between experimental measurements (Wexp), theoretical predictions (Wsim), and the adjusted model (Wsim, k) across all experimental runs. This comparison allows the evaluation of not only the predictive capability of the theoretical model, but also its ability to reproduce the temporal evolution of the evaporation–condensation process under real operating conditions.

The model reproduced the relative differences among runs, indicating that it provides a consistent representation of the available evaporative energy. The ratio between experimental and simulated production ranged from 0.36 to 0.43. For the adjusted model, the lower-bound value (k = 0.36) was used as a conservative empirical correction factor to avoid overestimating distillate production.

This pattern supported the use of an empirical, system-specific correction factor to adjust the magnitude of the theoretical predictions. After applying this factor, the adjusted model (Wsim_k) showed closer agreement with the experimental values; however, it should be interpreted as a preliminary calibration rather than as confirmation of model transferability or physical robustness. Since no independent validation dataset was available, the correction factor should not be considered transferable without further testing under broader operating conditions. The detailed numerical results are provided in Appendix B.

The hourly profiles reveal a diurnal pattern across all runs (Figure 8), characterised by a progressive increase in distillate production during the morning, peak values around midday (12:00–14:00 h), and a decline during the late afternoon. The observed response indicates that the system's thermal state is driven by incoming solar radiation, while evaporation depends more on the progressive build-up of energy within the unit than on momentary atmospheric conditions.

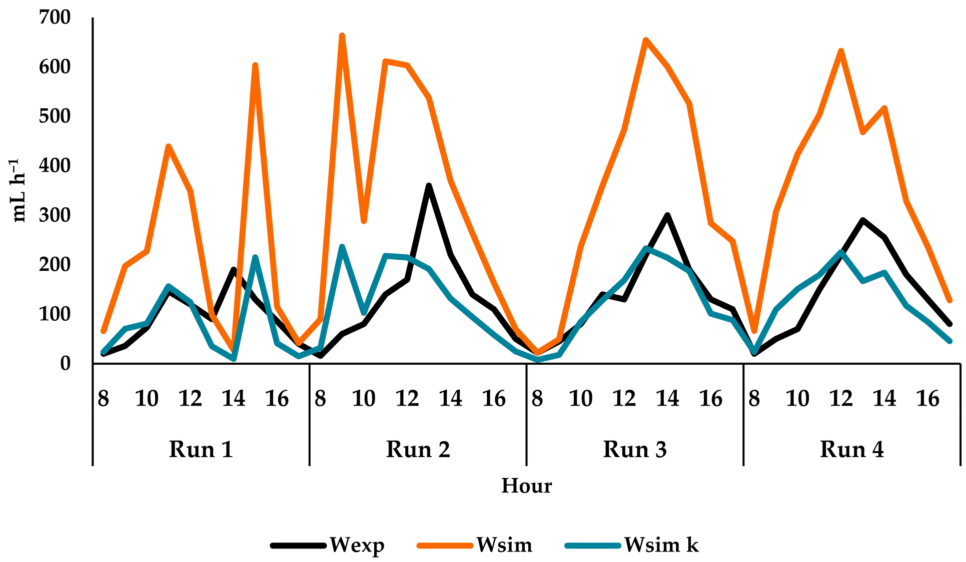

Figure 8. Experimental and simulated daily distillate production.

However, significant differences are observed between the theoretical and experimental results. The classical model (Wsim) overestimates distillate production throughout the day, with peak values exceeding experimental observations by up to two to three times. This overestimation is pronounced during periods of high thermal input, suggesting that the model assumes ideal heat transfer and complete conversion of thermal energy into evaporation.

In contrast, the adjusted model (Wsim_k) showed closer agreement with the experimental data in terms of magnitude and temporal pattern. Within the evaluated conditions, the correction factor helped reduce the discrepancy between theoretical and observed trends.

Despite the improvement, discrepancies persist at the hourly scale, during early morning and late afternoon, likely due to transient thermal effects such as energy storage, delayed water heating, and non-instantaneous condensation. Both the theoretical and adjusted models reproduced the main shape of the production curves, suggesting that the model structure captures the dominant thermal of the pilot system. Thus, limitations arise from unaccounted system inefficiencies rather than model formulation. Overall, the theoretical model captures system dynamics but overestimates production, while the correction factor enhances its applicability under real conditions.

The daily distillate production results summarised in Table 4 compare experimental measurements (Wexp), theoretical predictions (Wsim), and adjusted values (Wsim_k) across all experimental runs in mL·m^{-2}·day^{-1}. This comparison provides a preliminary assessment of model performance at the aggregated scale and supports the evaluation of its ability to represent evaporation-driven distillate production under the tested operating conditions.

Table 4. Experimental vs. simulated distillate daily production.

Run	Total Wexp	Total Classical Wsim	Total k-Adjusted Wsim k
1	931	2165.4	771.8
2	1346	3658.6	1304.0
3	1367	3452.3	1230.5
4	1445	3610.1	1286.7

The results show that the classical model overestimates distillate production by approximately two to three times relative to experimental values. However, after applying the correction factor, the adjusted model exhibits a close agreement with observed data, reducing deviations. This result suggests that the theoretical model represents the evaporative energy available in the pilot system, but it does so under idealised assumptions. Incorporating the correction factor allows real operating losses and inefficiencies to be reflected, thereby improving prediction at the daily scale.

The statistical performance of the theoretical and adjusted models is summarised in Table 5 using standard evaluation metrics, including MAE, RMSE, MAPE, and R^2. These indicators provide a quantitative assessment of model accuracy and bias, allowing comparison between the original formulation and the calibrated approach in representing daily distillate production under real operating conditions.

Table 5. Statistical performance of theoretical and adjusted models.

Model	MAE (mL day^{-1})	RMSE (mL day^{-1})	MAPE (%)	R^2
Classical model Wsim	1950	2035	148	0.64
Adjusted model Wsim k	60	75	5.0	0.64

The classical model showed high prediction errors, with MAPE reaching 148%, confirming a systematic overestimation of distillate production. The adjusted model improved the agreement with experimental data, reducing MAPE to 5% and lowering both MAE and RMSE. However, R^2 remained unchanged (0.64), indicating that the correction factor mainly adjusted the magnitude of the predictions rather than the temporal correlation structure. These results suggest that the main discrepancy was associated with the scale of the theoretical predictions under real operating conditions; however, additional datasets would be required to assess whether other structural sources of error are also present.

4. Discussion

Due to the limited number of operational runs, the comparison between passive and active modes should be interpreted as descriptive and indicative, rather than as evidence of statistically validated differences between operating modes.

Passive-mode productivity remained within the range reported by [22] for single-effect basin stills operating under favourable solar conditions. By contrast, the higher production achieved under active operation reflects the contribution of auxiliary thermal input, which enhances evaporation rates and reduces the system's dependence on instantaneous solar irradiance. This difference became evident under suboptimal meteorological conditions. During periods of cloud cover and light rainfall, the active configuration maintained production levels that exceeded passive-mode outputs under comparable conditions and approached those observed in passive mode under favourable weather, thereby indicating improved operational performance and reduced sensitivity to short-term weather variability [43].

This pattern can be explained by the thermodynamic mechanisms governing solar distillation. As reported by [20], the productivity of the pilot system is controlled by the temperature gradient between the basin water (Tw) and the inner surface of the glass cover (Tg). In the present study, active operation contributed to maintaining a more stable Tw–Tg differential, thereby sustaining evaporation and condensation rates over a longer portion of the diurnal cycle. This thermal stability appeared to reduce the system's dependence on instantaneous solar radiation and support a longer effective production window under variable climatic conditions.

From a treatment perspective, the physicochemical removal efficiencies achieved in this study fall within the performance range reported for solar-based wastewater treatment units [38,39] and approach the higher efficiencies documented in recent studies [40]. The reduction in COD and BOD to concentrations below the maximum permissible limits established by Colombian environmental regulation [34] suggests potential for controlled discharge of the treated effluent. Likewise, the removal of total suspended solids was consistent with previously reported values for solar distillation units treating domestic wastewater [38,39], supporting the role of the evaporation–condensation process in separating non-volatile suspended contaminants from the condensate. Nevertheless, these results should be interpreted as separation-driven improvements in condensate quality rather than evidence of contaminant mineralisation.

In microbiological terms, the near-complete removal of total and faecal coliforms is consistent with pathogen reduction levels reported in solar distillation of domestic sewage [26,41]. This performance is attributed to the combined effects of thermal inactivation and phase-change separation, which prevent microbial transfer into the condensate. Unlike conventional decentralised treatment systems based on biological or filtration processes, solar distillation operates as a physical barrier, reducing the need for additional disinfection stages.

Within this context, the integration of solar still unit as a polishing stage aligns with approaches reported for decentralised and low-cost wastewater treatment systems, such as horizontal flow constructed wetlands, which have demonstrated their suitability for reuse-oriented applications in small-scale scenarios [44].

The results suggest that, under the tested pilot-scale conditions, the active configuration may support the use of the solar still unit as a polishing component in decentralised treatment trains. Its capacity to improve effluent quality, contribute to regulatory compliance, and operate with relatively low energy requirements supports its applicability in rural and resource-limited contexts. This is consistent with recent studies highlighting the potential of combined biological and thermal separation processes as effective and sustainable strategies for wastewater treatment [45].

Within the conditions evaluated in this pilot study, the active mode appeared to support higher observed distillate production and greater apparent thermal stability, although further replicated trials are required to confirm this behaviour under broader operating conditions. Recent studies indicate that, although solar stills are simple and suitable for small-capacity or remote applications, their practical implementation remains constrained by low productivity, area requirements, and the need for design or operational optimisation [46,47]. However, its broader practical relevance will depend on future assessments of photovoltaic reliability, operating costs, maintenance requirements, total energy use in active mode, specific distillate yield per unit of energy input, and a complete water balance, including the volume and quality of the residual concentrate, where retained dissolved and particulate constituents may accumulate after evaporation [48]. While the distillation process can contribute to the separation of non-volatile contaminants and microorganisms, the potential transfer of volatile or semi-volatile compounds was not assessed in this study. This is particularly relevant for domestic wastewater, where ammonia, Volatile Organic Compounds (VOCs), cleaning agents, pharmaceuticals, personal care products, and other emerging contaminants may be present. Future studies should therefore include targeted analyses of these compounds in both the condensate and the residual concentrate [49,50].

The classical solar still model provides a physically consistent but idealised representation of distillate production. Its systematic overestimation indicates that part of the absorbed energy is not converted into useful evaporation in the pilot system. The correction factor ($k \approx 0.36$) can therefore be interpreted as an empirical parameter of the present SSU, accounting for the overall deviation between idealised model behaviour and observed performance. This value is consistent with efficiency ranges reported for solar still unit [51].

5. Conclusions

In this pilot study, the solar still unit showed potential to improve the physicochemical and microbiological quality of domestic wastewater condensate, with substantial reductions in COD, BOD, TSS, and microbial indicators. However, given the limited number of operational runs and the absence of analytical replicates, these findings should be interpreted as preliminary and system-specific. The results support its potential role as a polishing component within decentralised domestic wastewater treatment trains, rather than as a fully demonstrated stand-alone treatment solution. Nevertheless, its suitability for discharge or reuse should be confirmed through broader water-quality characterisation, including volatile, semi-volatile, and emerging contaminants not assessed in the present study. The passive operation mode exhibits greater sensitivity to meteorological variability, including cloud cover and precipitation, than active operation, which affects the daily volume of treated water.

Solar still performance is governed by an integrated energy balance, where daily aggregation better reflects unit response than hourly variability influenced by transient effects. The identified correction factor ($k \approx 0.36$) should be interpreted as an empirical adjustment for the present SSU and operating conditions, rather than as a universally transferable efficiency parameter. This framework bridges theory and practice while highlighting the influence of design and operational parameters such as insulation and geometry. Combining physical modelling with empirical calibration provides a useful approach for interpreting solar-still performance at the pilot scale for decentralised applications.

Author Contributions: Conceptualization, C.M.M., F.H.G., K.C.T. and O.O.P.; methodology, K.C.T., and C.M.M.; validation, S.S., A.A., M.D. and M.V.; formal analysis, C.M.M., F.H.G., S.S., A.A., M.D. and M.V.; investigation, C.M.M. and F.H.G.; resources, K.C.T. and O.O.P.; data curation, C.M.M.; writing—original draft, C.M.M. and F.H.G.; writing—review and editing, C.M.M., F.H.G., K.C.T., O.O.P., S.S., A.A., M.D. and M.V.; visualisation, C.M.M.; supervision, K.C.T., O.O.P., S.S., A.A., M.D. and M.V.; project administration, K.C.T.; funding acquisition, C.M.M. All authors have read and agreed to the published version of the manuscript.

Funding: This research received no external funding.

Data Availability Statement: The original contributions presented in this study are included in the article. Further inquiries can be directed to the corresponding authors.

Acknowledgments: The authors highlight that this paper was made possible thanks to the academic collaboration agreement between the Research Center on Appropriate Technologies for Environmental Management in Limited Resources Countries (CeTAmb) of the University of Brescia (Italy), the UNIPAZ Instituto Universitario de la Paz (Colombia) and the Peasant Association of the Cimitarra River Valley ACVC (Colombia). The authors would like to thank Ana Gutiérrez R., Andy Sanabria N., Anyi Arango P., and Diana Martínez M., students at UNIPAZ, for their theses in environmental engineering, which were important input for the present paper.

Conflicts of Interest: The authors declare no conflicts of interest.

Abbreviations

The following abbreviations are used in this manuscript:

SSU	Solar Still Unit
DWW	Domestic Wastewater
WWTP	Wastewater Treatment Plant
WWTS	Wastewater Treatment System
COD	Chemical Oxygen Demand
BOD	Biological Oxygen Demand
TSS	Total Suspended Solids
PCM	Phase Change Material
MAE	Mean Absolute Error
RMSE	Root Mean Square Error
MAPE	Mean Absolute Percentage Error
WASH	Water, Sanitation and Hygiene

Appendix A

Construction Start-up Untreated and treated water samples

Figure A1. Development and commissioning of a solar still unit.

Appendix B

Table A1. Passive mode dataset.

Run	Hour	I W m^{-1}	Ta °C	Tw °C	Tg °C	v m s^{-1}	Wexp mL h^{-1}	Wsim Classical mL h^{-1}	Wsim k-Adjusted mL h^{-1}
Run 1	8	280.9	26.6	37.0	31.5	2.0	20.0	65.8	23.5
Run 1	9	312.4	27.9	48.9	40.6	2.0	36.0	197.3	70.3
Run 1	10	474.3	30.8	52.8	44.9	2.0	73.0	227.3	81.0
Run 1	11	663.3	31.6	60.4	50.3	2.0	146.0	439.2	156.6
Run 1	12	670.3	31.6	55.4	45.1	2.0	120.0	349.2	124.5
Run 1	13	766.4	32.3	55.0	51.4	2.0	90.0	98.6	35.1
Run 1	14	790.7	33.4	59.9	58.8	2.0	190.0	27.5	9.8
Run 1	15	795.8	34.1	60.7	47.3	2.0	130.0	603.3	215.0
Run 1	16	244.6	32.6	43.3	36.6	2.0	86.0	115.5	41.2
Run 1	17	105.2	30.7	34.0	29.7	2.0	40.0	41.7	14.9
Run 2	8	242.7	26.6	33.6	25.2	2.0	16.0	89.8	32.0
Run 2	9	276.0	27.9	56.8	38.8	2.0	60.0	663.3	236.4
Run 2	10	458.0	30.8	56.1	47.7	2.0	80.0	288.0	102.7
Run 2	11	494.4	31.2	60.2	46.3	2.0	140.0	611.0	217.8
Run 2	12	512.6	31.6	63.0	51.0	2.0	170.0	602.8	214.8
Run 2	13	526.8	32.3	60.7	48.7	2.0	360.0	537.4	191.5
Run 2	14	569.3	33.4	59.5	50.5	2.0	220.0	369.3	131.6
Run 2	15	642.1	34.1	55.8	47.9	2.0	140.0	264.5	94.3
Run 2	16	295.0	32.6	49.0	42.0	2.0	110.0	162.9	58.1
Run 2	17	141.6	30.7	36.5	30.6	2.0	50.0	69.7	24.8
Run 3	8	184.0	29.5	23.9	19.9	2.0	22.0	22.0	7.9
Run 3	9	459.0	30.2	28.0	21.5	2.0	45.0	49.4	17.6
Run 3	10	538.9	31.5	45.7	34.3	2.0	80.0	237.4	84.6
Run 3	11	556.1	33.2	49.2	34.9	2.0	140.0	359.7	128.2
Run 3	12	592.5	35.4	57.3	44.8	2.0	130.0	473.1	168.6
Run 3	13	630.2	36.3	60.7	46.2	2.0	220.0	654.0	233.1
Run 3	14	651.2	36.3	64.4	53.2	2.0	300.0	600.1	213.9
Run 3	15	750.3	37.1	57.5	43.8	2.0	190.0	525.5	187.3
Run 3	16	388.3	36.3	50.9	40.4	2.0	130.0	283.8	101.2
Run 3	17	381.2	36.2	41.6	27.0	2.0	110.0	247.3	88.1
Run 4	8	267.9	27.6	34.4	28.2	2.0	20.0	66.1	23.6
Run 4	9	280.7	28.7	47.9	34.8	2.0	50.0	307.7	109.7
Run 4	10	697.7	31.3	55.8	43.7	2.0	70.0	423.8	151.1
Run 4	11	721.9	32.6	56.5	42.7	2.0	150.0	503.4	179.4
Run 4	12	775.5	34.3	62.1	49.0	2.0	220.0	632.1	225.3
Run 4	13	560.2	34.9	59.6	48.5	2.0	290.0	467.8	166.8
Run 4	14	801.8	35.3	61.0	49.6	2.0	255.0	516.4	184.1
Run 4	15	550.1	35.3	55.5	45.8	2.0	180.0	328.5	117.1
Run 4	16	489.4	35.4	49.7	40.3	2.0	130.0	236.3	84.2
Run 4	17	330.7	33.6	40.8	32.6	2.0	80.0	128.0	45.6

Note: Thermal model equations: P(T) = exp(25.317 − 5144/(T + 273.15)); P_w = exp(25.317 − 5144/(T_w + 273.15)); P_g = exp(25.317 − 5144/(T_g + 273.15)); h_cw = 0.884[(T_w − T_g) + (P_w − P_g)(T_w + 273.15)/(268,900 − P_w)]^(1/3); h_ew = 0.016273 h_cw ((P_w − P_g)/(T_w − T_g)); q_ew = h_ew (T_w − T_g); m_ew = (q_ew × 3600)/L_v; W_sim = m_ew × 1000.

References

1. Saravia Matus, S.; Gil Sevilla, M.; Fernández, D.; Montañez, A.; Blanco, E.; Naranjo, L.; Llavona, A.; Sarmanto, N. Oportunidades de la Economía Circular en el Tratamiento de Aguas Residuales en América Latina y el Caribe. 2022. Available online: https://repositorio.cepal.org/server/api/core/bitstreams/3413ec71-7292-4ce7-95a8-a6b4aa53faae/content (accessed on 1 April 2026).
2. Massoud May, A.; Tarhini, A.; Nasr, J.A. Decentralized approaches to wastewater treatment and management: Applicability in developing countries. *J. Environ. Manag.* **2009**, *90*, 652–659. [CrossRef]
3. Capodaglio, A.G. Integrated, decentralized wastewater management for resource recovery in rural and peri-urban areas. *Resources* **2017**, *6*, 22. [CrossRef]
4. Sha, C.; Shen, S.; Zhang, J.; Zhou, C.; Lu, X.; Zhang, H. A review of strategies and technologies for sustainable decentralized wastewater treatment. *Water* **2024**, *16*, 3003. [CrossRef]
5. SSPD, Superintendencia de Servicios Públicos Domiciliarios. *Estudio Sectorial de los Servicios Públicos de Acueducto y Alcantarillado–2025*; Superintendencia de Servicios Públicos Domiciliarios: Bogotá, Colombia, 2025. Available online: https://www.superservicios.gov.co/sites/default/files/2025-12/Informe-Sectorial-de-los-Servicios-Publicos-Domiciliarios-de-Acueducto-y-Alcantarillado-2024.pdf (accessed on 1 April 2026).
6. Colombia. Ministerio de Vivienda, Ciudad y Territorio. *Plan Nacional de Manejo de Aguas Residuales PMAR 2020–2050—1ra*; Ed/Viceministerio de Agua y Saneamiento Básico, Ed.; Ministerio de Vivienda, Ciudad y Territorio: Bogotá, Colombia, 2022; 60p. Available online: https://www.minvivienda.gov.co/publicacion/plan-nacional-de-manejo-de-aguas-residuales-municipales-pmar-2020-2050 (accessed on 1 April 2026).

7. DNP, Departamento Nacional de Planeación. Documento CONPES 3177 Consejo Nacional de Política Económica y Social República de Colombia. Acciones Prioritarias y Lineamientos para la Formulación del Plan Nacional de Manejo de Aguas Residuales. 2022. Available online: https://colaboracion.dnp.gov.co/CDT/Conpes/Econ%C3%B3micos/3177.pdf (accessed on 1 April 2026).
8. DNP, Departamento Nacional de Planeación. Documento CONPES 4004 Consejo Nacional de Política Económica y Social República de Colombia. Economía Circular en la Gestión de los Servicios de Agua Potable y Manejo de Aguas Residuales. 2020. Available online: https://colaboracion.dnp.gov.co/CDT/Conpes/Econ%C3%B3micos/4004.pdf (accessed on 1 April 2026).
9. DNP, Departamento Nacional de Planeación. Documento CONPES 3919 Consejo Nacional de Política Económica y Social República de Colombia. Política Nacional de Edificaciones Sostenibles. 2018. Available online: https://colaboracion.dnp.gov.co/CDT/Conpes/Econ%C3%B3micos/3919.pdf (accessed on 1 April 2026).
10. Liu, M.; Lin, Z.; Li, J.; Zhu, M.; Tang, Z.; Li, K. Performance assessment of rural decentralized domestic wastewater treatment facilities in Foshan, China. *Water* **2024**, *16*, 1901. [CrossRef]
11. Kumar, V.; Das, B.; Gupta, R.; Newar, P.P. Experimental evaluation of single-slope solar stills for municipal wastewater treatment using cement balls and iron chips as thermal energy storage materials. *J. Water Process Eng.* **2025**, *77*, 108369. [CrossRef]
12. Sifat, A.I.; Uddin, M.M. Water distillation method using solar power. *Mater. Today Proc.* **2017**, *4*, 314–321. [CrossRef]
13. Brandon, R.; Morris, T.C.; Fernández-Ibáñez, P.; McGuigan, K.G.; Heida, A.; Hamilton, K.A.; Khan, W. Decentralised solar-based water treatment—Bridging the last mile to water security in low- and middle-income countries? *Water Secur.* **2023**, *20*, 100146. [CrossRef]
14. Arunkumar, T.; Sathyamurthy, R.; Denkenberger, D.; Lee, S.J. Solar distillation meets the real world: A review of solar stills purifying real wastewater and seawater. *Environ. Sci. Pollut. Res.* **2022**, *29*, 22860–22884. [CrossRef] [PubMed]
15. Younis, O.; Hussein, A.K.; Attia, M.E.H.; Aljibori, H.S.S.; Kolsi, L.; Togun, H.; Ali, B.; Abderrahmane, A.; Subkrajang, K.; Jirawattanapanit, A. Comprehensive Review on Solar Stills—Latest Developments and Overview. *Sustainability* **2022**, *14*, 10136. [CrossRef]
16. Parsa, S.M.; Rahbar, A.; Koleini, M.H.; Aberoumand, S.; Afrand, M.; Amidpour, M. A renewable energy-driven thermoelectric-utilized solar still with external condenser loaded by silver/nanofluid for simultaneously water disinfection and desalination. *Desalination* **2020**, *480*, 114354. [CrossRef]
17. Tony, M.A.; Nabwey, H. A Recent advances in solar still technology for solar water desalination. *Appl. Water Sci.* **2024**, *14*, 147. [CrossRef]
18. Elsheikh, A.H.; Sharshir, S.W.; Ali, M.K.A.; Shaibo, J.; Edreis, E.M.A.; Abdelhamid, T.; Du, C.; Zhang, H. Thin film technology for solar steam generation: A new dawn. *Sol. Energy* **2019**, *177*, 561–575. [CrossRef]
19. Weixiang, C.; Pi, S.; Yang, Y.; Li, Z.; Yu, Y.; Yang, Y.; Yang, R.; Li, H.; Lu, L. Solar-Driven interfacial evaporation for decentralized direct potable reuse of domestic wastewater. *Chem. Eng. J.* **2023**, *468*, 143582. [CrossRef]
20. Sampathkumar, K.; Arjunan, T.V.; Pitchandi, P.; Senthilkumar, P. Active solar distillation—A detailed review. *Renew. Sustain. Energy Rev.* **2010**, *14*, 1503–1526. [CrossRef]
21. Rajaseenivasan, T.; Murugavel, K.K.; Elango, T.; Hansen, R.S. A review of different methods to enhance the productivity of the multi-effect solar still. *Renew. Sustain. Energy Rev.* **2013**, *17*, 248–259. [CrossRef]
22. Kumar, P.V.; Kumar, A.; Prakash, O.; Kaviti, A.K. Solar stills system design: A review. *Renew. Sustain. Energy Rev.* **2015**, *51*, 153–181. [CrossRef]
23. Kumar, P.M.; Sudarvizhi, D.; Prakash, K.B.; Anupradeepa, A.M.; Raj, S.B.; Shanmathi, S.; Sumithra, K.; Surya, S. Investigating a single slope solar still with a nano-phase change material. *Mater. Today Proc.* **2021**, *45*, 7922–7925. [CrossRef]
24. Chaichan, M.T.; Kazem, H.A.; Al-Waeli, A.H.; Elawee, W.H.; Fayad, M.A.; Sopian, K. Advanced techniques for enhancing solar distiller productivity: A review. *Energy Sources Part A Recovery Util. Environ. Eff.* **2024**, *46*, 736–772. [CrossRef]
25. Reddy, K.S.; Sharon, H.; Krithika, D.; Philip, L. Performance, water quality and enviro-economic investigations on solar distillation treatment of reverse osmosis reject and sewage water. *Sol. Energy* **2018**, *173*, 160–172. [CrossRef]
26. Soni, A.; Stagner, J.A. Adaptable wind/solar powered hybrid system for household wastewater treatment. *Sustain. Energy Technol. Assess.* **2017**, *24*, 8–18. [CrossRef]
27. Collivignarelli, M.C.; Gomez, F.H.; Caccamo, F.M.; Sorlini, S. Reduction of pathogens in greywater with biological and sustainable treatments selected through a multicriteria approach. *Environ. Sci. Pollut. Res.* **2023**, *30*, 38239–38254. [CrossRef] [PubMed]
28. Gomez, F.H.; Collivignarelli, M.C.; Bellazzi, S.; Torres, K.C.; Abbà, A.; Sorlini, S. Sequential Treatment of Domestic Wastewater in Rural Zones Applying Aloe Vera Extract as Coagulant (Preliminar), E. crassipes in a Horizontal Biofilter (Secondary), and Activated Carbon from Soursop Seeds (Tertiary). *Clean Technol.* **2025**, *7*, 105. [CrossRef]
29. IDEAM. Normales Climatológicas 1991–2020. 2024. Available online: http://www.ideam.gov.co/web/tiempo-y-clima/clima (accessed on 1 April 2026).
30. IDEAM. Atlas de Radiación Solar, UV y Ozono de Colombia. 2024. Available online: http://www.ideam.gov.co/web/tiempo-y-clima/atlas-de-colombia (accessed on 1 April 2026).

31. Meza, C.M.; Torres, K.C.; Porras, O.O.; Racero, I.L.; Paredes, M.R.; Corredor, F.; Aguilar, Y. *Identificación y Valoración de los Servicios Ecosistémicos en la Zona Alta del DRMI Humedal San Silvestre*; Libro Resultado de Investigación; Instituto Universitario de la Paz (UNIPAZ): Barrancabermeja, Colombia, 2024.
32. Patel, P.; Solanki, A.S.; Soni, U.R.; Patel, A.R. A review to increase the performance of solar still: Make it multi layer absorber. *Int. J. Recent Innov. Trends Comput. Commun.* **2014**, *2*, 173–177. Available online: https://api.semanticscholar.org/CorpusID:212503934 (accessed on 1 April 2026).
33. APHA; AWWA; WEF. *Standard Methods for the Examination of Water and Wastewater*, 24th ed.; Section 2540 D (Total Suspended Solids Dried at 103–105 °C), Section 5210 B (Biochemical Oxygen Demand), Section 5220 C (Chemical Oxygen Demand); American Public Health Association: Washington, DC, USA, 2023.
34. Resolution 631 of 2015. Colombian Environmental Regulation. Por la Cual se Establecen los Parámetros y los Valores Límites Máximos Permisibles en los Vertimientos Puntuales a Cuerpos de Aguas Superficiales y a los Sistemas de Alcantarillado Público y se Dictan Otras Disposiciones. Available online: https://www.minambiente.gov.co/wp-content/uploads/2021/11/resolucion-631-de-2015.pdf (accessed on 1 April 2026).
35. Medugu, D.W.; Ndatuwong, L.G. Theoretical analysis of water distillation using solar still. *Int. J. Phys. Sci.* **2009**, *4*, 705–712.
36. Gupta, B.; Mandraha, T.K.; Edla, P.J.; Pandya, M. Thermal modeling and efficiency of solar water distillation: A review. *Am. J. Eng. Res.* **2013**, *2*, 203–213.
37. Willmott, C.J.; Matsuura, K. Advantages of the mean absolute error (MAE) over the root mean square error (RMSE) in assessing average model performance. *Clim. Res.* **2005**, *30*, 79–82. Available online: http://www.jstor.org/stable/24869236 (accessed on 1 April 2026). [CrossRef]
38. Asadi, R.Z.; Suja, F.; Ruslan, M.H. The application of a solar still in domestic and industrial wastewater treatment. *Sol. Energy* **2013**, *93*, 63–71. [CrossRef]
39. Igoud, S.; Zeriri, D.; Aoudjit, L.; Boutra, B.; Sebti, A.; Khene, F.; Mameche, A. Climate change adaptation by solar wastewater treatment (SOWAT) for reuse in agriculture and industry. *Irrig. Drain.* **2021**, *70*, 243–253. [CrossRef]
40. Yusof, M.F.; Zainol, M.R.R.M.A.; Riahi, A.; Zakaria, N.A.; Shaharuddin, S.; Juiani, S.F.; Noor, N.M.; Zawawi, M.H.; Ikhsan, J. Investigation on the Urban Grey Water Treatment Using a Cost-Effective Solar Distillation Still. *Sustainability* **2022**, *14*, 9452. [CrossRef]
41. Kumar, M.; Patel, S.K.; Mishra, V.; Singh, D.; Singh, D. Sustainable approach for wastewater treatment by using passive type single basin double slope solar still. *Indian Chem. Eng.* **2025**, 1–17. [CrossRef]
42. Kumar, V.; Das, B.; Gupta, R.; Newar, P.P. An experimental investigation on sustainable desalination of lake and municipal wastewater using a thermal storage–assisted single-slope solar still. *Environ. Sci. Pollut. Res.* **2025**, *32*, 27242–27262. [CrossRef] [PubMed]
43. Abujazar, M.S.S.; Fatihah, S.; Rakmi, A.R.; Shahrom, M.Z. The effects of design parameters on productivity performance of a solar still for seawater desalination: A review. *Desalination* **2016**, *385*, 178–193. [CrossRef]
44. Collivignarelli, M.C.; Carnevale Miino, M.; Gomez, F.H.; Torretta, V.; Rada, E.C.; Sorlini, S. Horizontal flow constructed wetland for greywater treatment and reuse: An experimental case. *Int. J. Environ. Res. Public Health* **2020**, *17*, 2317. [CrossRef] [PubMed]
45. Gomez, F.H.; Collivignarelli, M.C.; Bellazzi, S.; Torres, K.C.; Sorlini, S.; Vaccari, M. Mercury removal from mining wastewater by bioaccumulation and thermal separation in Eichhornia crassipes. *Environ. Sci. Pollut. Res.* **2025**, *32*, 798–810. [CrossRef] [PubMed]
46. Kumar, S.; Ahmad, A.; Irshad, K.; Prakash, O.; Kausher, R.; Hasnain, S.M.M.; Pandey, S.; Tapalova, A.; Akylbekov, N.; Zairov, R. Solar stills: A review for water scarcity solutions. *Heliyon* **2024**, *10*, e38751. [CrossRef] [PubMed]
47. Khalaf, M.O.; Özdemir, M.R.; Sultan, H.S. A Comprehensive Review of Solar Still Technologies and Cost: Innovations in Materials, Design, and Techniques for Enhanced Water Desalination Efficiency. *Water* **2025**, *17*, 1515. [CrossRef]
48. Hanson, A.; Zachritz, W.; Stevens, K.; Mimbela, L.; Polka, R.; Cisneros, L. Distillate water quality of a single-basin solar still: Laboratory and field studies. *Sol. Energy* **2004**, *76*, 635–645. [CrossRef]
49. Song, C.; Qi, D.; Han, Y.; Xu, Y.; Xu, H.; You, S.; Wang, W.; Wang, C.; Wei, Y.; Ma, J. Volatile-Organic-Compound-Intercepting Solar Distillation Enabled by a Photothermal/Photocatalytic Nanofibrous Membrane with Dual-Scale Pores. *Environ. Sci. Technol.* **2020**, *54*, 9025–9033. [CrossRef] [PubMed]
50. Oluwole, A.O.; Omotola, E.O.; Olatunji, O.S. Pharmaceuticals and personal care products in water and wastewater: A review of treatment processes and use of photocatalyst immobilized on functionalized carbon in AOP degradation. *BMC Chem.* **2020**, *14*, 62. [CrossRef] [PubMed]
51. Tiwari, G.N.; Singh, H.N.; Tripathi, R. Present status of solar distillation. *Sol. Energy* **2003**, *75*, 367–373. [CrossRef]